Approaches to the Solution NMR Characterization of Active Sites for 65 kDa Tetrameric Hemoglobins in the Paramagnetic Cyanomet State

Urszula Kolczak, Chang Han, L. A. Sylvia, and Gerd N. La Mar*

Contribution from the Department of Chemistry, University of California, Davis, California 95616

Received July 3, 1997. Revised Manuscript Received October 15, 1997[⊗]

Abstract: A solution ^{1}H 2D NMR investigation has been carried out on low-spin, human adult cyanomet hemoglobin (HbA) to elucidate molecular, electronic, and magnetic properties of the heme cavities in the hetero-tetrameric globin. It is shown that, in spite of its size, 65 kDa, and paramagnetism ($S = {}^1/_2$), appropriately tailored 2D experiments to suppress rotating frame dipolar correlation allow detection of the scalar connectivities needed to identify heme and heme pocket residue spin topology, as well as the backbone $^3J(\alpha\text{-N})$ necessary to assign residues sequence-specifically. NOESY rise curves clearly differentiate between primary and secondary NOEs and afford the sensitivity for providing interproton distance estimates. The combined NMR strategies provide the complete assignment of the heme, a key portion of the F-helix, the F-G turn, and residues in contact with ligands. Unambiguous subunit differentiation for all signals was achievable independently, either sequence-specifically via the Ala$^\alpha$ *vs* Cys$^\beta$ at position F9 or by conserved heme C-helix contacts for Tyr$^\alpha$ *vs* Phe$^\beta$ at position C7. The dipolar shifts for the assigned heme pocket residues provide the orientation of the anisotropic paramagnetic susceptibility tensor in the molecular framework, showing that the major axis in each subunit is tilted from the heme normal by ∼11° in a direction consistent with a bound cyanide exhibiting a tilt from the heme normal similar to that as observed for CO in the HbACO crystal. Numerous identified residues have been implicated in the mechanism of cooperativity. Analysis of the dipolar contacts between the heme vinyl and/or propionate groups with the adjacent heme methyls and neighboring protein residues identifies different 6-propionate mobility in the two subunits and 4-vinyl orientations with out-of-plane orientations to opposite sides of the heme in the two subunits. It is concluded that homonuclear 2D NMR is capable of providing unique information on functionally relevant structural and dynamic properties of HbA in the cyanomet form in spite of its size and paramagnetism; in fact, the paramagnetism facilitates the structural studies by significantly improving spectral resolution for the heme cavity.

Introduction

The ligand affinities for O_2 and CO in monomeric hemoglobin (Hb)[1] and myoglobin (Mb) are exquisitely modulated over wide ranges by relatively few residues within a largely conserved globular fold consisting of 7−8 helices with the heme wedged between helices E and F and ligated by His(F8).[2] Various direct influences have been proposed to modulate the stability of the ligated *vs* unligated protein, including hydrogen-bond stabilization by the ubiquitous His(E7) of the bound O_2 (observed in neutron diffraction of MbO_2),[3] steric destabilization by Val(E11) for bound CO (observed by tilt or bend of Fe-CO in X-ray diffraction of MbCO[4] or HbCO[5]), and pocket polarity as determined by residues such as B10.[6] A more indirect mechanism proposed to modulate ligand affinity in general is the control of the spacing between the F-helix and the heme, which must be significantly reduced in ligated *vs* unligated states.[7] The control of ligand affinity in the vertebrate hetero-tetrameric Hb, $\alpha_2\beta_2$, is modulated in a complex manner by a variety of allosteric effectors that include protons (Bohr effect), subunit ligation (cooperativity), and CO_2, organic phosphate, and chloride binding at sites remote from the heme;[2,8] only NO binding in the β subunit is close to the heme cavity (Cys$^\beta$93(F9)).[9] The influence of these allosteric effectors has been visualized by X-ray crystallography as resulting from changes in the position for the equilibrium between two alternate quaternary states, the low-affinity, "tense" or T-state exhibited by deoxy Hb, and the high-affinity, "relaxed" or R-state which exhibits significantly altered inter-subunit contacts.[7,10] The exact mechanisms by which the altered inter-subunit contacts are transmitted to the heme within each subunit, however, is incompletely understood, although a logical pathway from the subunit interface to the axial His(F8) and Val(FG5) in contact with pyrrole B of the heme has been proposed.[2,7,11,12]

[⊗] Abstract published in *Advance ACS Abstracts,* December 1, 1997.

(1) Abbreviations used: HbA, human adult hemoglobin; metHbACN, cyanide-ligated ferric HbA; HRP, horseradish peroxidase; 2D, two dimensional; NOE, nuclear Overhauser effect; NOESY, two-dimensional nuclear Overhauser spectroscopy; TOCSY, two-dimensional total correlation spectroscopy; COSY, two-dimensional bond correlation spectroscopy; DSS, 2,2-dimethyl-2-silapentane-5-sulfonic acid; ppm, parts per million.

(2) Dickerson, R. E.; Geis, I. *Hemoglobin: Structure, Function, Evolution, and Pathology*; Benjamin/Cummings: Menlo Park, CA, 1983.

(3) Phillips, S. E. V.; Schoenborn, B. P. *Nature (London)* **1981**, *292*, 81−82.

(4) Kuriyan, J.; Wilz, S.; Karplus, M.; Petsko, G. A. *J. Mol. Biol.* **1986**, *192*, 133−154.

(5) Baldwin, J. M. *J. Mol. Biol.* **1980**, *136*, 103−128.

(6) Springer, B. A.; Sligar, S. G.; Olson, J. S.; Phillips, G. N. *Chem. Rev.* **1994**, *94*, 699−714.

(7) Perutz, M. F. *Mechanisms of Cooperativity and Allosteric Regulation in Proteins*; Cambridge University Press: Cambridge, England, 1990.

(8) Antonini, E.; Brunori, M. *Hemoglobin and myoglobin in their reactions with ligands*; North-Holland Pub. Co.: Amsterdam, 1971.

(9) Mylvaganam, S. E.; Bonaventura, C.; Bonaventura, J.; Getzoff, E. D. *Nat. Struct. Biol.* **1996**, *3*, 275−283.

(10) Perutz, M. F.; Fermi, G.; Luisi, B.; Shaanan, B.; Liddington, R. C. *Acc. Chem. Res.* **1987**, *20*, 309−321.

(11) Gelin, B. R.; Lee, A. W.; Karplus, M. *J. Mol. Biol.* **1983**, *171*, 489−559.

S0002-7863(97)02213-0 CCC: $14.00

In principle, ^{1}H NMR can provide detailed information on the heme cavity structure for the diamagnetic O_2 and CO complexes of ferrous Mb and Hb.[13,14] In practice, the size of even monomeric globins (~150 residues) severely complicates the needed unique assignments in the absence of ^{15}N labeling.[15] The intrinsic paramagnetism ($S = {}^1/_2$) of monomeric metHbCN and metMbCN provides a strong advantage for defining steric tilt and H-bonding to bound ligand because the large magnetic anisotropy induces significant dipolar shifts for heme pocket residues. These shifts greatly facilitate the detection and spatial placement of the labile protons involved in H-bonding. The orientations of the major magnetic axis and rhombic axes reflect largely the tilt of the Fe-CN unit and orientation of the axial His(F8) magnetic side chain, respectively, relative to the heme plane.[16−23] The inevitable enhanced relaxation due to the paramagnetism complicates, but does not preclude,[24] the 2D NMR characterization relative to a diamagnetic system. In fact, the increased spectral dispersion due to the hyperfine shifts can compensate for the enhanced relaxation so as to simplify the assignment and spatial placement of distal residue relative to a diamagnetic analog.[23]

^{1}H NMR studies of tetrameric Hb have been largely confined to 1D experiments where the His(F8) $N_\delta H$ contact shift in deoxy Hb and/or the inter-subunit hydrogen bonds in any Hb ligation/oxidation state could be correlated to the quaternary structure (for reviews, see refs 12 and 25). Early 1D NMR analysis of hyperfine-shifted signals of metHbCN had proposed some resonance assignments for heme resonances based on comparison to metMbCN and model compounds and correlated the subunit origin of such resonances using valency hybrids[26] or naturally occurring mutants.[27] Limited definitive heme assignment resulted from reconstitution of individual subunits with selective deuterated hemes.[28] Very limited 2D NMR of diamagnetic HbCO have identified portions of the heme and several distal residue signals using the crystal structure as a guide to the identity of the residue and the subunit origin of both the heme and amino acid residues.[29] In fact, detailed NMR characterization has been largely restricted to the isolated α-chain which is monomeric at low pH.[13,30,31] The extension of 2D NMR approaches from the monomeric metMbCNs to the tetrameric metHbCN complex is complicated by much more serious spectral congestion due to the presence of two subunits, as well as the broader resonances and stronger cross relaxation for the larger size (~65 kDa), which undermines detection of scalar correlation, enhances the ROESY response,[32] and exacerbates spin-diffusion in NOESY spectra.[33]

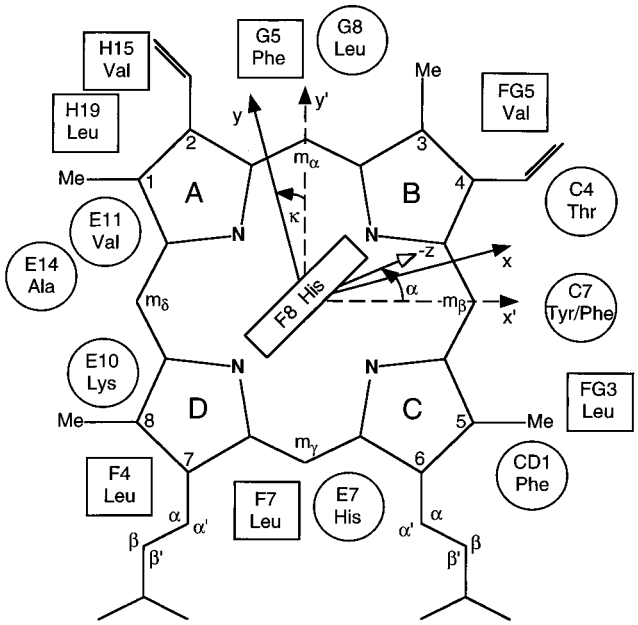

Figure 1. Schematic representation of the heme pocket for the two subunits of HbA with residues on the proximal (squares) and distal (circles) residue expected to contact the heme. The heme positions are labeled in the Fischer notation, and the residues are identified by their conserved helical (*i.e.*, F8) or turn (*i.e.*, FG3) positions. The x', y', z' coordinate system represents an iron-centered coordinate system derived from the crystal coordinates of HbACO. The magnetic axes, x, y, z, in which the paramagnetic susceptibility tensor is diagonal, are related by the Euler rotation $\Gamma(\alpha, \beta, \gamma)$ via $(x, y, z) = (x', y', z')\ \Gamma(\alpha, \beta, \gamma)$, where β represents the tilt of the major magnetic axis from the heme normal, α is the direction of this tilt, defined as the angle between the projection of the $-z$-axis on the x', y' plane and the x'-axis, and $\kappa \approx \alpha + \gamma$ locates the projection of the rhombic axes onto the heme plane.

In the interest of extending detailed molecular and electronic structural studies to the allosteric vertebrate Hb, we focus in this paper on the assessment of the efficacy of 2D NMR for unambiguous assignment and structure characterization of the 65 kDa adult human metHbCN complex in a manner profitably pursued for isoelectronic monomeric Hb and Mb complexes.[17−22] We use the cyanomet complex of human adult Hb, metHbACN, since numerous subunit-specific heme assignments are available from earlier isotope labeling studies[28] and these resonances can serve as the test for the effectiveness for a solely 2D NMR approach to subunit-specific assignment in similar tetrameric Hbs. A schematic representation of the heme and nearby target residue is shown in Figure 1. The questions we address in this report are the following: How effective are the available homonuclear 2D NMR methods for assigning and spatially

(12) Ho, C. *Adv. Prot. Chem.* **1992**, *43*, 153−312.
(13) Dalvit, C.; Ho, C. *Biochemistry* **1985**, *24*, 3398−3407.
(14) Dalvit, C.; Wright, P. E. *J. Mol. Biol.* **1987**, *194*, 313−327. Dalvit, C.; Wright, P. E. *J. Mol. Biol.* **1987** *194*, 329−339.
(15) Theriault, Y.; Pochapsky, T. C.; Dalvit, C.; Chiu, M. L.; Sligar, S. G.; Wright, P. E. *J. Biomol. NMR* **1994**, *4*, 491−504.
(16) Shulman, R. G.; Glarum, S. H.; Karplus, M. *J. Mol. Biol.* **1971**, *57*, 93−115.
(17) Emerson, S. D.; La Mar, G. N. *Biochemistry* **1990**, *29*, 1556−1566.
(18) Rajarathnam, K.; La Mar, G. N.; Chiu, M. L.; Sligar, S. G. *J. Am. Chem. Soc.* **1992**, *114*, 9048−9058. Rajarathnam, K.; Qin, J.; La Mar, G. N.; Chiu, M. L.; Sligar, S. G. *Biochemistry* **1993**, *32*, 5670−5680. Rajarathnam, K.; Qin, J.; La Mar, G. N.; Chiu, M. L.; Sligar, S. G. *Biochemistry* **1994**, *33*, 5493−5501.
(19) Qin, J.; La Mar, G. N.; Ascoli, F.; Brunori, M. *J. Mol. Biol.* **1993**, *231*, 1009−1023.
(20) Qin, J.; La Mar, G. N.; Cutruzzolá, F.; Travaglini Allocatelli, C.; Brancaccio, A.; Brunori, M. *Biophys. J.* **1993**, *65*, 2178−2190.
(21) Zhao, X.; Vyas, K.; Nguyen, B. D.; Rajarathnam, K.; La Mar, G. N.; Li, T.; Phillips, G. N., Jr.; Eich, R. F.; Olson, J. S.; Ling, J.; Bocian, D. F. *J. Biol. Chem.* **1995**, *270*, 20763−20774.
(22) Zhang, W.; La Mar, G. N.; Gersonde, K. *Eur. J. Biochem.* **1996**, *237*, 841−853.
(23) Wu, Y.; Basti, M.; Chiancone, E.; Ascoli, F.; La Mar, G. N. *Biochim. Biophys. Acta* **1996**, *1298*, 261−275.
(24) La Mar, G. N.; de Ropp, J. S. *Biol. Magn. Reson.* **1993**, *18*, 1−78.
(25) Ho, C.; Perussi, J. R. *Methods Enzymol.* **1994**, *232*, 97−139.
(26) Ogawa, S.; Shulman, R. G.; Yamane, T. *J. Mol. Biol.* **1972**, *70*, 291−300. Ogawa, S.; Shulman, R. G.; Fujiwara, M.; Yamane, T. *J. Mol. Biol.* **1972**, *70*, 301−313.
(27) Davis, D. G.; Charache, S.; Ho, C. *Proc. Natl. Acad. Sci. U.S.A.* **1969**, *63*, 1403−1409.
(28) La Mar, G. N.; Jue, T.; Nagai, K.; Smith, K. M.; Yamamoto, Y.; Kauten, R. J.; Thanabal, V.; Langry, K. C.; Pandey, R. K.; Leung, H.-K. *Biochim. Biophys. Acta* **1988**, *952*, 131−141.
(29) Craescu, C. T.; Mispelter, J. *Eur. J. Biochem.* **1989**, *181*, 87−96
(30) Martineau, L.; Craescu, C. T. *Eur. J. Biochem.* **1992**, *205*, 661−670.
(31) Martineau, L.; Craescu, C. T. *Eur. J. Biochem* **1993**, *214*, 383−393.
(32) Griesinger, C.; Otting, G.; Wüthrich, K.; Ernst, R. R. *J. Am. Chem. Soc.* **1988**, *110*, 7870−7872.
(33) Cavanagh, J.; Fairbrother, W. J.; Palmer, A. G., III; Skelton, N. J. *Protein NMR Spectroscopy*; Academic Press: San Diego, CA, 1996.

defining residues in such a large and paramagnetic complex? Can the complete heme unit be assigned without recourse to isotope labeling? Can the subunit origin of both the heme and heme pocket residue signals be uniquely determined without recourse to valency hybrids or explicit use of the crystal structure? Can the resulting hyperfine shifts be interpreted in terms of the molecular structure of Hb? Do these NMR data provide new information on the structural differences between the subunits? The ultimate goal is to be able to determine by NMR the heme cavity structure of tetrameric Hb mutant human or other natural genetic variants to the same detail now attainable for monomeric Mb[17−21] and Hb.[22] The effect of quaternary structure on the ^{1}H NMR spectral parameters of the cyanomet state can be investigated in the valency hybrids of HbA, (deoxy-α-chain)$_2$(met-β-chain-CN)$_2$ and (met-α-chain-CN)$_2$(deoxy-β-chain)$_2$ which can be induced to undergo the allosteric transition.[26,34]

Experimental Section

Sample Preparation. HbA was isolated and purified by standard procedures.[8] Packed human red blood cells, obtained from a local blood center, were diluted 1:2 with 1% NaCl solution and washed four times by centrifugation at 4 °C for 30 min at 500*g*. The red cells were suspended in two volumes of cold distilled water and kept at 4 °C overnight. The HbA was separated from lysed cells by centrifugation at 5000*g* for 2 h. CyanomethemoglobinA, metHbACN, was prepared by oxidation of the oxyhemoglobin with potassium ferricyanide, followed by chromatography on a G-25 column equilibrated with 20 mM Tris HCl, 20 mM NaCl, and 10 mM KCN (pH 8.0). Prior to NMR measurement, the metHbACN solution was buffer exchanged and concentrated in an Amicon ultrafiltration cell to a final concentration ∼2 mM in 20 mM NaCl, 40 mM KCN, and 50 mM sodium phosphate, pH 8.4; 10% ^2H_2O was added to the ^1H_2O solutions for the spectrometer lock.

NMR Spectra. All ^{1}H NMR spectra were collected on a GE Ω 500 spectrometer operating at 500 MHz. Chemical shift values were referenced to DSS through the residual water signal. Reference 1D spectra were collected by the one-pulse with H_2O presaturation, super-WEFT,[35] or modified DEFT (90°−τ−180°−τ−90°) techniques.[36] The nonselective T_1 values for the resolved peaks were obtained as previously described in detail.[37] For paramagnetically dominated T_1 values, the distance from the iron for proton i was estimated via T_1(H$_i$)/T_1(heme-CH$_3$) = R^6(Fe-H$_i$)/R^6(Fe-CH$_3$), using R = 6.1 Å and T_1 ≈ 130 ms for the heme 1-CH$_3$.

Phase-sensitive 2D NOE (NOESY)[38] were collected over the temperature range of 25−45 °C for ^2H_2O sample over a spectral window of 20.0 kHz using 2048 points in the acquisition dimension (t_2); 160 scans were collected for each of 512 evolution (t_1) increments with mixing time τ_m = 35 ms. The recycle time was 300 ms. The NOESY spectra ^1H_2O sample were collected at 45 °C over 20.0 kHz with τ_m = 35 ms and a 250 ms recycle time, or over 15.0 kHz with τ_m = 45 ms and recycle time of 500 ms. The COSY spectrum[39] was recorded in the magnitude mode over 12.0 kHz with a 250 ms recycle time. The clean-TOCSY[32] spectra were collected over 15.0 kHz with τ_m = 20 ms (^1H_2O) and 12.0 kHz with τ_m = 12 ms (^2H_2O) and a 500 ms or 250 ms recycle time. The SCUBA method[40] was used to recover intensity of saturated C$_\alpha$H resonances resulting from irradiation of the solvent line during the relaxation delay. The NOESY buildup curves were based on NOESY data sets with τ_m = 3.3−30 ms. In all 2D experiments, quadrature detection in t_1 employed the hypercomplex method of States *et al.*[41] All 2D data were processed on a Silicon Graphics workstation using the software package Felix from Biosym/MSI (San Diego). Data sets were processed with 20−40°-shifted sine-bell-squared apodization in both dimensions and phase-corrected and base-line-straightened in both dimensions.

Magnetic Axes Determination. The magnetic axes were determined as described in detail previously.[17,18] Experimental dipolar shifts for the structurally conserved residues in both subunits were used as input to search for the Euler rotation angles α, β, γ, that transform the molecular pseudosymmetry coordinates, x', y', z' (or r, θ', Ω') (Figure 1) obtained from crystal coordinates into the magnetic axes, x, y, z, (or r, θ, ϕ) by minimizing the following error function:

$$F/n = \sum |\delta_{dip}(\text{obsd}) - \delta_{dip}(\text{calcd})F(\alpha,\beta,\gamma)|^2 \quad (1)$$

where

$$\delta_{dip}(\text{calcd}) = {}^1/_{3N}[\Delta\chi_{ax}(3\cos^2\theta' - 1)r^{-3} + {}^3/_2(\Delta\chi_{rh}\sin^2\theta'\cos 2\Omega')r^{-3}] \quad (2)$$

with

$$\delta_{dip}(\text{obsd}) = \delta_{DSS}(\text{obsd}) - \delta_{DSS}(\text{dia}) \quad (3)$$

$\Delta\chi_{ax}$ and $\Delta\chi_{rh}$ are the axial and rhombic anisotropies; δ_{DSS}(dia) is the shift in the isostructural diamagnetic HbCO[29] or isolated α-chain, α-CO.[30] For the protons in the β-subunit, the δ_{dia} from α-subunit were used or were calculated by using the equation: $\delta_{DSS}(\text{dia}) = \delta_{sec} + \delta_{rc}$, where δ_{sec} is the shift of an amino acid proton typical for the α-helices, β-strand, coils, etc., and δ_{rc} is the heme-induced ring current shift based on the HbACO coordinates[5] by using the eight-loop model.[42]

Results

(A) Reference Spectra. The resolved portions of the normal 500 MHz ^{1}H NMR spectrum of metHbACN in ^2H_2O at 37 °C is shown in Figure 2A. Heme peaks are labeled by the position in the Fischer notation (1−8, α-*δ*-*meso*; see Figure 1), while amino acid residues, because of differences in sequence numbers from homologous residues, is given by their position on the helix (*i.e.*, His(F8) is the 8th residue on the F-helix) or turn (*i.e.*, Val(FG5) is the 5th residue on the FG turn). The α- and β-subunit origins are differentiated by labeling the β-subunit peaks by asterisks based on subunit-specific assignment determined below. Lower or higher temperature resolves the two 5-CH$_3$ peaks, but results in other degeneracies (data not shown; see the Supporting Information). A combination of a DEFT spectrum to enhance the intensity of strongly relaxed protons, together with deconvolution that improves resolution, affords the reference spectrum in Figure 2B that locates several intense, paramagnetically affected resonances under the aromatic envelope, emphasizes a series of moderately relaxed, single-proton signals in the −0.5 to −2.5 ppm window, and reveals the presence of at least five separate signals under the composite centered at −3 ppm, which exhibits an intensity of ∼15 proton in the normal reference spectra. The 12−16 ppm portion of a super-WEFT spectrum (Figure 2C) effectively suppresses intensity of all peaks with T_1 > 100 ms and clearly demonstrates the presence of two strongly relaxed Phe(CD1) C$_\zeta$H resonances, which are difficult to detect in Figure 2A,B. The combined analysis over the 15−45 °C range identifies a total of 39 (25 low-field, 14 upfield) resolved to partially resolved nonlabile proton signals. Comparison of the low-field portion of the ^{1}H NMR spectra of metHbACN in ^2H_2O (Figure 3A) with those in ^1H_2O collected with a 1:1 pulse train without (Figure 3B) or with (Figure 3C) saturation of the ^1H_2O signal identifies strongly

(34) Shibayama, N.; Morimoto, H.; Saigo, S. *Biochemistry* **1997**, *36*, 4375−4381.
(35) Inubushi, T.; Becker, E. D. *J. Magn. Reson.* **1983**, *51*, 128−133.
(36) Hochmann, J.; Kellerhals, H. J. *J. Magn. Reson.* **1980**, *38*, 23−29.
(37) Emerson, S. D.; La Mar, G. N. *Biochemistry* **1990**, *29*, 1545−1556.
(38) Jeener, J.; Meier, B. H.; Bachmann, P.; Ernst, R. R. *J. Chem. Phys.* **1979**, *71*, 4546−4553.
(39) Bax, A. T. *Two-Dimensional NMR in Liquids*; Reidel Publishing Co.: Dordrecht, The Netherlands, 1982.
(40) Brown, S. C.; Weber, P. L.; Mueller, L. *J. Magn. Reson.* **1988**, *77*, 166−169.
(41) States, D. J.; Haberkorn, R.; Ruben, D. *J. Magn. Reson.* **1982**, *48*, 286−296.
(42) Cross, K. J.; Wright, P. E. *J. Magn. Reson.* **1985**, *64*, 220−231.

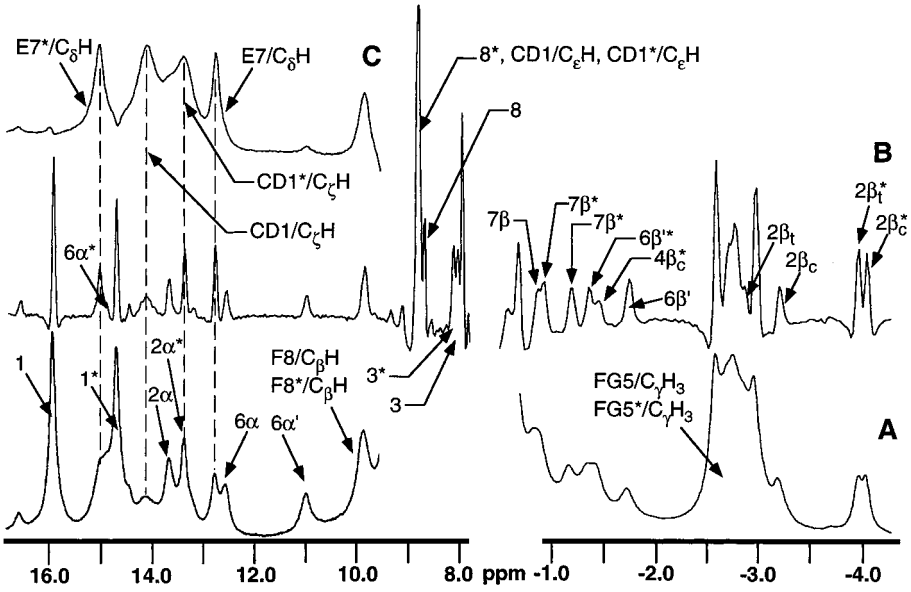

Figure 2. Resolved portions of the 500 MHz ^{1}H NMR spectra of metHbACN in ^2H_2O, 20 mM in NaCl, at 37 °C: (A) reference spectrum with solvent presaturation, collected at 4 scans/s and apodized with exponential 3 Hz line broadening; (B) deconvoluted (10° shifted-sine-bell-squared) DEFT spectrum (relaxation delay 100 ms collected at 4 scans/s) that improves resolution with minimal loss of intensity from broad peaks; and (C) WEFT spectrum (relaxation delay 60 ms, collected at 4 scans/s) that emphasizes the two most strongly relaxed ($T_1 \approx 20$ ms) nonlabile proton peak for Phe(CD1) C$_\zeta$Hs.

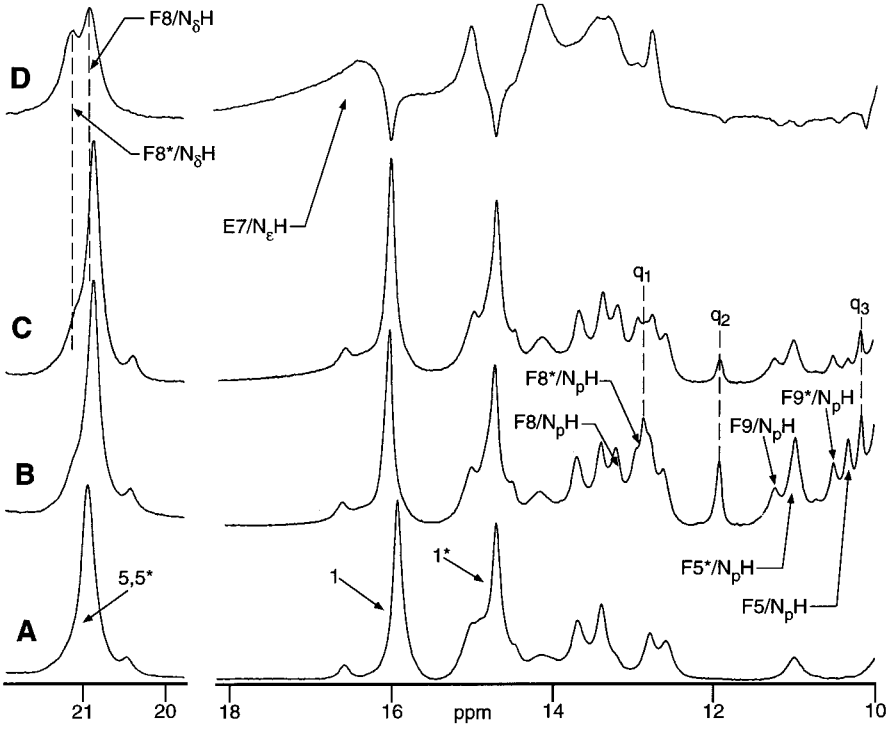

Figure 3. Low-field resolved portions of the 500 MHz ^{1}H NMR spectra of metHbACN, 20 mM in NaCl, at 37 °C collected with a 1:1 pulse train with solvent presaturation in ^2H_2O (A), and in 90% ^1H_2O:10% ^2H_2O without (B) and with (C) solvent presaturation. Labile protons are detected in (B) at full intensity and in (C) with some partially saturated by exchange with water. (D) WEFT-spectrum (relaxation delay 30 ms, 4 scans/s) of a 90% ^1H_2O:10% ^2H_2O solution which identifies a rapidly relaxed ($T_1 \approx 20$ ms) labile proton at ~16.5 ppm not observed in ^2H_2O and emphasizes the two strongly relaxed proton signal under the composite at 21 ppm.

relaxed labile proton signals under the 5-CH$_3$ peak, as well as nine other labile protons to the low-field region of 10 ppm, several of which exhibit saturation transfer due to exchange with the bulk solvent signal.[43] A partially relaxed spectrum at 40 °C (Figure 3D) identifies an additional strongly relaxed ($T_1 \approx$ 20 ms) labile proton on the left shoulder of the low-field 1-CH$_3$ peak.

(43) Sandström, J. *Dynamic NMR Spectroscopy*; Academic Press: NY, 1982; pp 53−59.

(B) Scalar Correlation. The efficacy of scalar correlation for metHbACN is relevant to our current goals in two contexts. One is the detection of the spin connectivity within the heme substituent vinyl and propionate groups and the axial His C$_\beta$Hs that, while experiencing significant relaxation, also exhibit relatively large spin coupling constants. The other is the need to detect J^3(N-α) for sequence-specific assignments which, because of the small value in α-helices, challenges their detection in even a diamagnetic 65 kDa protein.[44] Slices of

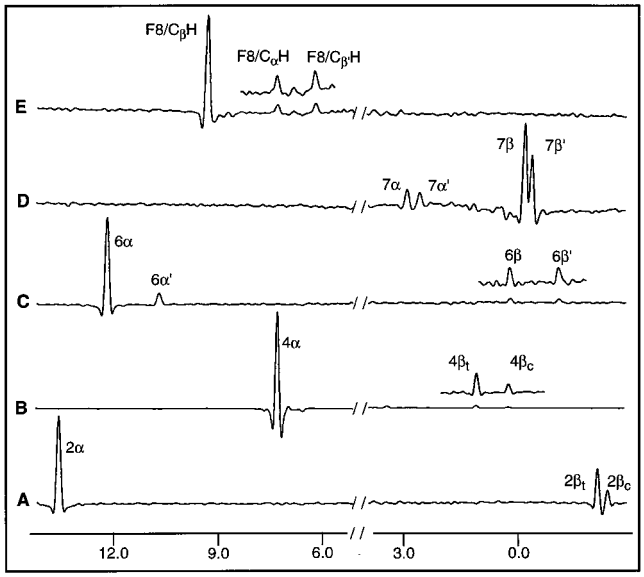

Figure 4. Slices of the clean-TOCSY spectrum (20 ms spin lock time) for the α-subunit of metHbACN in ^2H_2O, 20 mM NaCl at 45°C through the diagonals of the (A) 2-vinyl H_α, (B) 4-vinyl H_α, (C) 6-propionate H_α, (D) 7-propionate H_β, and (E) His(F8) $C_\beta H$ showing the complete scalar connectivity expected for each group.

the $\tau_m = 20$ ms TOCSY spectra for the α-subunit (the same peaks are observed for the β-subunit, not shown) heme vinyl (Figure 4A,B) and propionate (Figure 4C,D) side chains show the characteristic cross peak pattern as observed in either monomeric metMbCN[37] or MbCO.[45] Also shown in Figure 4E is the backbone spin connectivity for the (to be assigned) axial His(F8) C_βHs. The strong ROESY response of the opposite phase could be effectively suppressed using a strong spin-lock field and the clean-TOCSY variant.[32] Several of the resolved labile protons exhibit relatively strong TOCSY cross peaks to nonlabile protons with chemical shifts characteristic of low-field dipolar-shifted $C_\alpha H$ signals. The N_pH-$C_\alpha H$ fragment for the key axial His(F8) (shown in Figures 5B and 5D) experiences the strongest paramagnetic influence on relaxation and shifts. The TOCSY spectrum in Figure 5B, moreover, allows the detection of both cross peaks for a very strongly relaxed Phe ring (to be shown as Phe(CD1)).

A magnitude COSY spectrum of metHbACN reveals a pattern of cross peaks (data not shown; see the Supporting Information) involving relaxed and hyperfine-shifted protons that completely parallels the TOCSY cross peak pattern (Figure 4), with two exceptions. The vinyl $H_{\beta t}-H_{\beta c}$ COSY peaks are intense with respect to the small (~2 Hz) spin coupling, and a COSY cross peak is observed between (to be assigned) Val(FG5) $C\gamma H_3$ and $C_\alpha H$ of the α-subunit, in spite of negligible spin coupling (data not shown; see the Supporting Information). The latter two cross peaks indicate that cross correlation[46] contributes to COSY cross peaks and dictates a reliance on TOCSY for scalar correlation.

(C) Dipolar Correlation. NOESY maps collected with 3.3−30 ms mixing times exhibit numerous cross peaks for resolved resonances, including ones involving resonances with $T_1 \approx 20$ ms. A series of slices through the 5-CH_3 peaks reveals a majority of detectable primary cross peaks to the 5-CH_3 (data not shown; see the Supporting Information). Rise curves involving the 5-CH_3/6-propionate protons in the two subunits are illustrated in Figure 6A, which clearly differentiate between primary ($6H_\alpha \rightarrow$ 5-CH_3, $6H_\alpha \rightarrow 6H_\alpha'$) and secondary ($6H_\alpha' \rightarrow$ 5-CH_3) NOESY cross peaks and allow the stereospecific assignments of the individual propionate protons. Rise curves for the key Phe(CD1) ring (primary to H_ϵs, secondary to H_δs) and key Phe/Tyr(C7) rings (primary to H_δs; secondary to H_ϵs) contacts to the 5-CH_3 peaks are shown in Figure 6B.

(D) Resonance Assignments. Assignments are pursued along two lines: detection of unique spin topology for residues or fragments of residues with highly characteristic dipolar contact to the heme, as expected solely on the basis of the highly conserved folding topology of globins, optimally pursued in ^2H_2O, and, to the degree possible, standard backbone assignment in ^1H_2O as generally performed on small diamagnetic[47] or paramagnetic[48] proteins. The former strategy demands the complete and unambiguous assignment of the heme resonances, and the latter strategy is facilitated by independent identification of the axial His(F8) backbone. These assignments are greatly facilitated by the fact that at least some resonances for both the axial His and the heme exhibit significantly large and characteristic contact shifts so as to resolve them from the diamagnetic envelope; all of the chemical shifts are highly temperature dependent.[48,49]

The Heme. TOCSY spectra yield four three-spin (two resolved) and four four-spin (two partially resolved) systems involving relaxed and hyperfine-shifted protons that must arise from two vinyl and two propionate groups from each subunit (Figure 4). Two sets of heme methyls peaks are resolved and two additional sets are seen superimposed on the aromatic window but are better emphasized in Figure 2B. Relevant NOESY cross peaks for dipolar contacts are shown in the Supporting Information. NOESY cross peaks between hyperfine-shifted heme methyls identify 1-CH_3 and 8-CH_3, and the NOESY cross peaks from one to a vinyl and the other to a propionate differentiate 1-CH_3 and 8-CH_3 and identify the 2-vinyl and 7-propionate for one subunit. The NOESY cross peak from the 2-vinyl to another heme methyl, and the dipolar connection of that methyl to another vinyl, identify the 3-CH_3 and 4-vinyl. NOESY cross peaks between the 4-vinyl and a methyl, which in turn, shows dipolar contact to a propionate identify the 5-CH_3 and 6-propionate for one subunit. Lastly, NOESY cross peaks to a strongly relaxed hyperfine-shifted signal under the diamagnetic envelope by the residue adjacent to each meso position locate the α-, β-, γ-, and δ-*meso*-H signals (which also exhibit extreme low-field intercepts in a Curie plot). Parallel NOESY cross peaks similarly describe the complete second subunit heme. The heme chemical shifts at 37 °C and the slopes in a Curie plot (shift versus reciprocal temperature) for each subunit are given in Table 1.

Axial His(F8). One $C_\beta H$ and the ring $N_\delta H$ are invariably resolved for the axial His in all low-spin ferric hemoproteins. TOCSY spectra reveal two $C_\beta H_2 C_\alpha H$ fragments in ^2H_2O with one $C_\beta H$ near 10 ppm (Figure 5B), of which the C_αHs each exhibit a TOCSY cross peak in ^1H_2O (Figure 5D) to a resolved labile proton peak near 13 ppm (N_pH). The two strongly relaxed labile proton peaks under the 5-CH_3 composite, moreover, exhibit NOESY cross peaks to both the C_βHs and N_pH (Figure 5E), confirming the former assignment as the His(F8) N_δHs

(44) Gardner, K. H.; Rosen, M. K.; Kay, L. E. *Biochemistry* **1997**, *36*, 1389−1401. Yamazaki, T.; Tochio, H.; Furui, J.; Aimoto, S.; Kyogoku, Y. *J. Am. Chem. Soc.* **1997**, *119*, 872−880.

(45) Mabbutt, B. C.; Wright, P. E. *Biochim. Biophys. Acta* **1985**, *832*, 175−185.

(46) Bertini, I.; Luchinat, C.; Tarchi, D. *Chem. Phys. Lett.* **1993**, *203*, 445−449. Qin, J.; Delaglio, F.; La Mar, G. N.; Bax, A. *J. Magn. Reson. Ser. B* **1993**, *102*, 332−336.

(47) Wüthrich, K. *NMR of proteins and nucleic acids*; Wiley: New York, 1986.

(48) Qin, J.; La Mar, G. N. *J. Biomol. NMR* **1992**, *2*, 597−618.

(49) Bertini, I.; Turano, P.; Vila, A. J. *Chem. Rev.* **1993**, 93, 2833−2932.

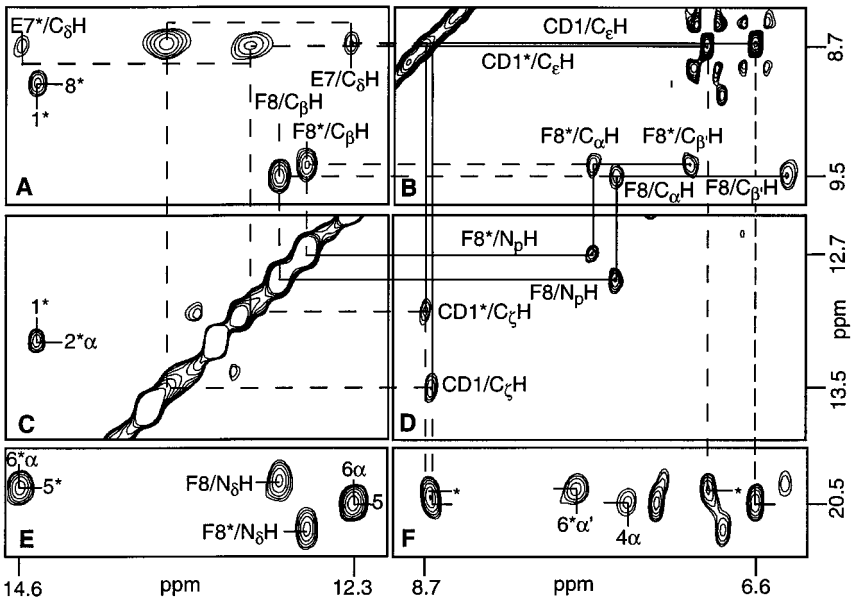

Figure 5. Portions of the NOESY spectrum (τ_m = 35 ms) (A, C, E, F) and clean-TOCSY spectrum (τ_m = 20 ms) (B, D) for metHbACN in 90% ^1H_2O:10% ^2H_2O, 20 mM in NaCl at 45 °C, illustrating the scalar connectivities for the backbone of His(F8) and the side chain of Phe(CD1) (B, D), the NOE between the His(F8) N_δHs and peptide NHs (E), the dipolar connection between the Phe(CD1) C_ϵH and His(E7) C_δHs (A), and the dipolar contact between the Phe(CD1) ring and the heme 5-CH_3 (F).

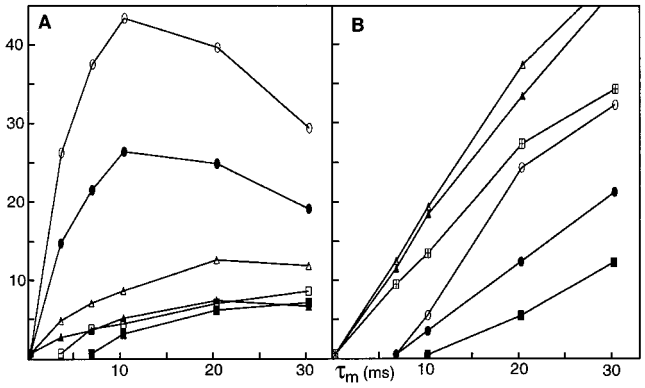

Figure 6. NOESY rise curves for the intensity, in arbitrary units, of the cross peak (A) through the 6H_α to 6H_α' (circle); 6H_α to 5-CH_3 (triangle); 6H_α' to 5-CH_3 (square); open markers designate the α-subunit, and closed markers the β-subunit; (B) through Phe/Tyr(C7) CH_δs (triangle) to 5-CH_3; Phe/Tyr(C7) C_ϵHs (square) to 5-CH_3, Phe(CD1) C_δHs (circle) to 5-CH_3 and Phe(CD1) C_ϵHs to 5-CH_3 (diamond; the signals for the two subunits are degenerate) open markers α-subunit, closed markers β-subunit. Note the primary NOE to Phe/Tyr(C7) C_δHs and Phe(CD1) H_ϵs.

for each subunit. The very broad peak of indeterminate intensity centered at 17 ppm, and detected only in the SUPER-WEFT trace (data not shown; see the Supporting Information), is typical for the axial His C_δH and/or C_ϵHs peak. The chemical shifts are listed in Table 2.

Conserved Heme Contacts with Diagnostic Spin Connectivity. The complete assignment of the heme and axial His(F8) signals for both subunits leave eight low-field (single proton) and four upfield (methyl) hyperfine-shifted and relaxed nonlabile proton resonances to be assigned in ^2H_2O solution. TOCSY (Figure 5B,D) and NOESY (Figure 5A) cross peaks for a low-field hyperfine-shifted residue with Curie intercepts in the aromatic window identify two Phe rings with strongly relaxed C_ζH ($T_1 \approx 20$ ms, $R_{Fe} \approx 4.4$ Å), and NOESY cross peaks between the ring and the 5-CH_3 signal (Figure 5F) identify Phe(CD1) for the respective subunits. The remaining four upfield, apparent methyl peaks exhibit TOCSY (Figure 7A) and NOESY (Figure 7B) cross peaks characteristic of a pair of

Table 1. ^{1}H NMR Spectral Parameters for the Heme in metHbACN

	α-subunit		β-subunit	
proton	chemical shift[a]	Curie slope[c]	chemical shift[a]	Curie slope[c]
1-CH_3	15.91(130)[b]	4.91	14.7(120)[b]	3.87
3-CH_3	8.04	−0.28	8.13	−1.79
5-CH_3	20.89(85)	4.69	20.89(85)	6.03
8-CH_3	8.68	−1.13	8.84	−1.47
2-H_α	13.66(115)	−0.19	13.35(115)	1.60
2-$H_{\beta c}$	−3.21	−4.47	−4.03	−4.56
2-$H_{\beta t}$	−2.88	−3.81	−3.99	−4.55
4-H_α	7.26	−1.68	5.65	−3.18
4-$H_{\beta c}$	−0.20	−1.98	−1.45	−3.04
4-$H_{\beta t}$	0.73	−1.59	−0.57	−2.51
6-H_α	12.53(100)	2.59	14.88(92)	4.05
6-H_α'	10.99(100)	1.02	7.59	−2.01
6-H_β	−0.24	−1.29	−0.03	−0.65
6-H_β'	−1.75	−2.42	−1.38	−1.86
7-H_α	2.27	−2.67	4.09	−1.64
7-H_α'	2.55	−3.63	0.97	−4.08
7-H_β	−0.61	−1.75	−0.90	−1.51
7-H_β'	−0.84	−1.93	−1.18	−1.88
α-meso-H	1.81	−3.32	2.43	−3.82
β-meso-H	4.78	−2.41	3.08	−5.04
γ-meso-H	4.52	−4.73	4.19	−3.98
δ-meso-H	2.24	−3.57	2.08	−4.58

[a] Chemical shift in ppm from DSS at 37 °C in ^2H_2O, 50 mM NaCl, pH 8.6. [b] T_1, in ms, with ±15% uncertainty, determined from the initial slope in an inversion-recovery experiment, is given in parentheses. [c] Slope in a plot of chemical shift versus reciprocal absolute temperature (Curie plot).

complete valines. The NOESY cross peaks for each of these valines to the 3-CH_3 (Figure 7D), 4-vinyl (Figure 7B,C,D), and 5-CH_3 (Figure 7E) are unique for the Val(FG5) for each subunit.

The use of TOCSY/NOESY spectra over a range of temperature provides the assignments for highly conserved residues in contact with the pyrrole A/D junction. TOCSY exhibit two cross peaks for two complete Ala, including the N_pH, with significant upfield dipolar shifts for the methyl, and with strong NOESY cross peaks to both the heme 1-CH_3 and 8-CH_3, that are diagnostic for Ala(E14) for each subunit. A second pair of resonances with strong upfield dipolar shifts which exhibit

Table 2. ^{1}H NMR Spectral Parameters for Heme Pocket Residues in metHbACN

		chemical shift[b] (T_1)[c]	
residue[a]	proton	α-subunit	β-subunit
Leu(B10)	$C_\gamma H$	4.56	4.23
	$C\delta_1H_3$	6.47	6.49
	$C\delta_2H_3$	5.17	5.36
Tyr/Phe(C7)	$C_\delta H$	5.87	6.03
	$C_\epsilon H$	5.62	6.38
	$C_\zeta H$		6.67
Phe(CD1)	$C_\delta H$	6.63	6.93
	$C_\epsilon H$	8.78	8.78
	$C_\zeta H$	14.11(20)	13.39(20)
Phe(CD4)	$C_\zeta H$	6.86	*d*
	$C_\epsilon H$	7.33	*d*
His(E7)	$C_\beta H$	3.70	4.27
	$C_\beta H'$	4.33	4.64[e]
	$C_\delta H$	12.78(45)	14.99(45)
Lys(E10)	NpH	6.36	*d*
	$C_\beta H$ (?)[f]	−0.55	−0.22
Val(E11)	$C_\alpha H$	−0.28	0.32
	$C_\beta H$	2.03	3.17
	$C\gamma_2H_3$ (?)[f]	3.23	2.00
Ala(E14)	NpH	6.80	6.60
	$C_\alpha H$	3.62	3.70
	$C_\beta H_3$	0.09	−0.08
Leu(F4)	N_pH	8.85	
	$C_\alpha H$	7.39	6.92
	$C_\beta H$	3.65	3.29
Ser(F5)	N_pH	10.31	10.95
	$C_\alpha H$	7.03	6.96
	$C_\beta H$	5.34	5.11
	$C_\beta H$	5.08	5.41
Asp/Glu(F6)	N_pH	9.28	9.19
	$C_\alpha H$	5.32	4.86
	$C_\beta H$	3.58	3.08
	$C_\beta H$	3.58	2.99
Leu(F7)	N_pH	9.62	9.79
	$C_\alpha H$	5.71	5.53
	$C_\beta H$	6.10	5.69
	$C_\beta H'$	3.68	3.53
	$C\delta_1H_3$	1.48	1.48
His(F8)	N_pH	13.17	12.92
	$C_\alpha H$	7.68	7.90
	$C_\beta H$	9.91(70)	9.79(70)
	$C_\beta H'$	6.12	6.63
	$N_\delta H$	20.85(40)	21.20(40)
Ala/Cys(F9)	N_pH	11.16	10.48
	$C_\alpha H$	5.26	5.09
	$C_\beta H_3/C_\beta H_S$	1.91	2.36, 3.04
Leu(FG3)	$C_{\delta1}H_3$	0.20	0.20
	$C_{\delta2}H_3$	0.44	0.63
Val(FG5)	N_pH	7.05	7.94
	$C_\alpha H$	2.22	2.41
	$C_\beta H$	0.11	0.58
	$C\gamma_1H_3$	−2.98(95)	−2.61(95)
	$C\gamma_2H_3$	−2.72(120)	−2.81(120)
Phe(G5)	$C_\delta Hs$	5.21	4.93
	$C_\epsilon Hs$	4.22	5.63
	$C_\zeta H$	7.61	7.92
Val(H15)	$C_\beta H$	*d*	1.65
	$C\gamma_1H_3$	*d*	−0.36

[a] In cases where homologous residues differs in the two subunits, the residue is identified α-subunit/β-subunit. [b] Chemical shift, in ppm from DSS in ^1H_2O, 50 mM NaCl, pH 8.4 a 37 °C. [c] T_1 estimate (±30%) for the null in intensity ($T_1 = \tau_{null}/\ln 2$) in an inversion-recovery experiment. [d] Not assigned. [e] At 45 °C. [f] The (?) denotes tentative assignment.

NOESY cross peaks, one each, to the 1-CH_3 and 8-CH_3 for each subunit and a TOCSY peak to one additional proton, uniquely identify the Val(E11) $C_\alpha H$-$C_\beta H$ fragment for both subunits. A cross peak to the 1-CH_3 with a significant (∼4−5 ppm) dipolar shift locates a candidate[50] for $C_{\gamma2}H_3$. A NOESY cross peak between the 3-CH_3 and a TOCSY-connected, moderately relaxed, and upfield-shifted proton with Curie-plot intercepts near 7 ppm for each subunit locates two aromatic rings, one each in contact with each of the 3-CH_3, and uniquely identifies the Phe(G5) for the respective subunits[51] (data not shown). The subunit-differentiated heme signals thus allow the assignment of all heme contact residues to one or the other subunit. For His(F8) with no heme contact, the His(F8) $C_\beta H$ NOESY cross peaks to the subunit-differentiated Val(FG5) $C_\gamma H_3$ provide the subunit differentiation. The chemical shifts and T_1 values (for resolved resonances) are listed in Table 2.

The various heme protons exhibit numerous NOESY cross peaks to the aliphatic window characteristic of methyl protons. Aside from one additional key aromatic contact (see below), the majority of the expected remaining heme contacts are to the termini of five Leu (F4, F7, FG3, G8, H19), one Val(H15), and one Thr(C4). In most cases, logical *candidates* for the methyls could be identified, but spectral congestion precluded definitive assignment. These assignments are very likely attainable with a range of mixing times for both TOCSY and NOESY spectra over a broad range of temperatures[48] and at a higher field strength. Moreover, since some tentative methyl assignments suggest that the side chain termini are often mobile and probably involves alternate orientations (see below), the assignment of the remaining aliphatic side chain protons was not pursued further at this point.

Subunit Origin by Conserved Heme−Protein Contacts. Inspection of the HbA sequence, together with the classical Mb fold characteristic of all known globins,[2] reveals that one highly conserved heme contact, namely that between residue C7 and the heme 5-CH_3 and 4-vinyl, differs for the two subunits, with the position occupied by Tyr42 in the α-subunit and Phe41 in the β-subunit. The heme 5-CH_3 and 4-vinyl for each subunit make dipolar contact with protons with Curie intercepts in the aromatic spectral window (Figure 8A,B,D) that are diagnostic for aromatic rings. TOCSY connectivities for the aromatic window (Figure 8C) identify two-spin and three-spin aromatic rings as origins for the aromatic contacts to two 5-CH_3 peaks, assignable to a Tyr and Phe side chain, respectively. These observations unequivocally identify the subunit with and without asterisks, as the β- and α-subunits, respectively. The chemical shifts are listed in Table 2.

Sequence- and Subunit-Specific Assignments by Backbone Connectivities. The key fingerprint portions of the metHbACN NOESY and TOCSY spectra are generally crowded, but the observation of four peptide NHs with a substantial low-field bias allows the detection of several helical fragments (Figure 9B,C). Seven-member (**I**) and Six-member (**I***) N_i−N_{i+1} segments are observed in the low-field NOESY spectrum (Figure 9B,C), for which TOCSY identifies the α- and β-protons for all but the last in segment **I**, and for which the i+4 residue is the His(F8) for the α-subunit identified above. The assigned His(F8) $N_\delta H$ exhibits the expected NOESY cross peaks to $C_\alpha H$ of Leu(F4). The residues exhibit the α_i−N_{i+1}, β_i−N_{i+1}, α_i−β_{i+3}, and/or α_i−N_{i+3} NOESY connectivities characteristic for a helix[47] for all but the last residues. The sequence identifies **I** as comprising residues 83−89, of which all but His89(FG1) (with NH at 8.52 ppm) are on the F-helix; noteworthy is the identification of Ala94(F9) at position i+5

(50) The line widths expected for the Val(E11) methyls due to their proximity to the iron likely preclude detection of TOCSY cross peaks to the $C_\beta Hs$.

(51) Only one TOCSY cross peak is detected for the Phe(G5) ring in the α-subunit. The assignment of the $C_\zeta H$ was based on the dipolar contacts to the $C_\epsilon H$ of Phe(G5) and methyl group of Val(FG5) and consistent slope of Curie plot with observed dipolar shift.

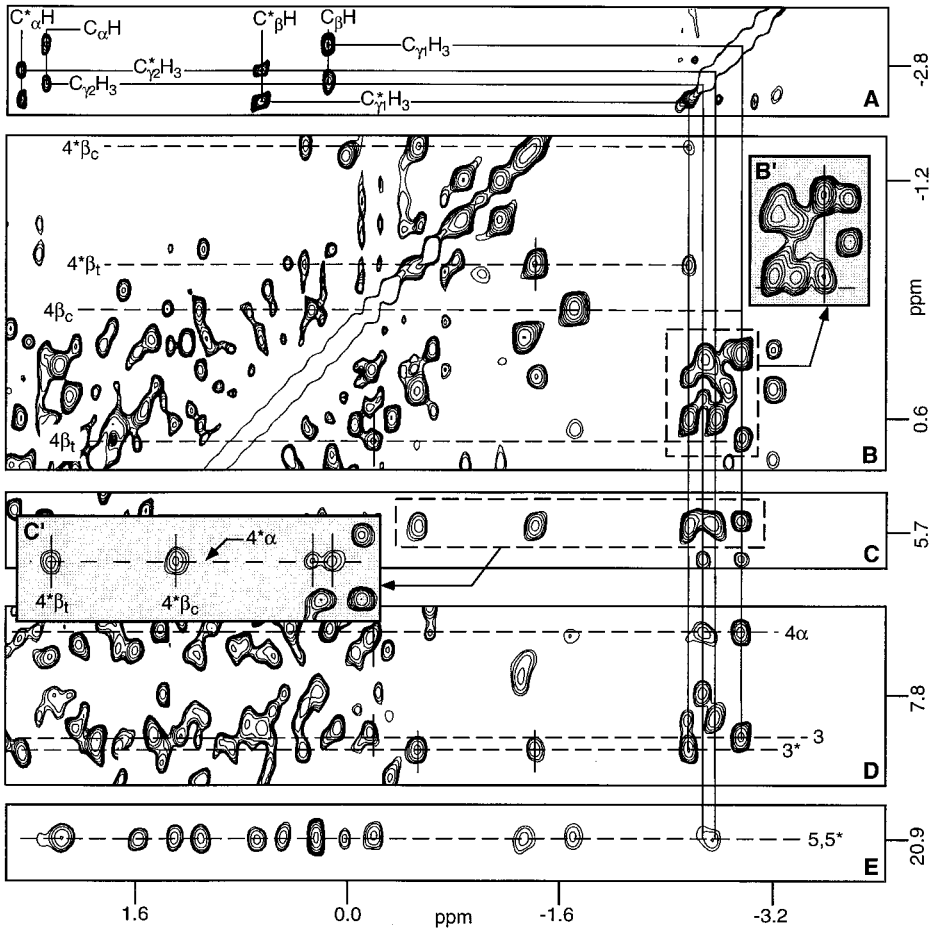

Figure 7. Portions of the clean-TOCSY ($\tau_m = 12$ ms) (A) and NOESY ($\tau_m = 35$ ms) (B−E) spectrum of metHbACN in ^2H_2O, 20 mM NaCl at 37 °C, illustrating the scalar connectivity for two complete Val(FG5) (A), the Val(FG5) NOESY connection to the 4-vinyl (B, C), 3-CH_3 (D) and 5-CH_3 (E) signals for the respective subunits. The shaded inserts B′ and C′ show the portion of the NOESY spectra at 25 °C that demonstrate that no cross peaks were observed between 4-vinyl H_βs and Val(FG5) in the α-subunit (B′ and B) and the 4-vinyl H_α shows a stronger cross peak to the methyl groups of Val(FG5) in α- (D) than in the β-subunit (C′).

which uniquely identifies segment **I** as arising from the α-subunit (completely independent of the separate identification of His(F8)).

Segment **I*** exhibits N-α, α-β TOCSY cross peaks for each residue, i*+1 to i*+5, and a α-β cross peak for i*; the N_i-α_i peak is too weak due to exchange of the NH. Again, α_{i*}−N_{i*+1}, β_{i*}−N_{i*+1}, α_{i*}−N_{i*+3} and α_{i*}−β_{i*+3} NOESY cross peaks to i*+4 establish the helical nature of segment **I***, with i*+5 due to Asp(FG1) (with NH shift 8.74 ppm). While the Leu(F4) NH could not be located, likely due to exchange, the α_{i*-1}−N_i, α_{i*-1}−β_{i+2} NOESY cross peaks locate the Leu C_αH, and a TOCSY cross peak identifies one of the C_βH. The Leu(F4) C_αH peak is again confirmed by the expected NOESY cross peak to the N_δH of the His(F8) ring. Since only the β protons are assigned for the F6 residue in the two subunits, the Asp/Glu*(F6) sequence differences between the subunits cannot be established for the residue at this time. Further tracing of NH−NH cross peaks of the F-helices is severely complicated by spectral congestion. Spectral congestion precluded identification at this time with certainty the backbone of the E-helix, even though the Ala(E14) NH in both subunits and the Lys(E10) NH of the α-subunit could be identified by characteristic heme contact.

The remaining four low-field labile protons exhibit significant saturation transfer and negligible paramagnetic relaxation, and the chemical shifts of two of them, q_1 (12.81 ppm) and q_2 (11.88 ppm) (see Figure 3B), are very similar to those for inter-subunit-hydrogen-bonding protons identified previously for diamagnetic HbA complexes.[52] A NOESY cross peak for q_1 to one of two spin-coupled aromatic protons (7.39, 6.92 ppm) identifies the Tyr35(C1) ring of the β-subunit H-bonded to Asp126(H9) of the α-subunit.[52] Similarly, peak q_2 exhibits strong NOESY cross peaks to two narrow signals in the aromatic spectral window without TOCSY connectivity (at 6.63, 8.04 ppm) that identify His103(G10) of the α-subunit that is H-bonded to the Asn108-(G10) of the β-subunit.[53] Peaks q_3 (10.13 ppm) and q_4 (9.98 ppm) (see Figure 9C) exhibit TOCSY/NOESY cross peaks diagnostic for two unassigned Trp indole rings.

Assignments Based on the Crystal Structure. These studies were pursued only to identify the functionally relevant His(E7) signals and to test the use of magnetic axes predictions as a guide for other assignments. The distal His(E7) is expected to place its ring protons close to the iron and the Phe(CD1) ring. Two remaining low-field resolved nonlabile proton peaks with no scalar connectivity, and with $T_1 \approx 45$ ms ($R_{Fe} \approx 5.6$ Å), exhibit a NOESY cross peak each to the two Phe(CD1) rings, as expected only for the His(E7) ring C_δH in each subunit (Figure 5A); NOESY cross peaks to the C_δHs locate candidates for the C_βHs. The ^{1}H NMR spectrum in ^1H_2O provides evidence for one low-field shifted and strongly relaxed labile proton ($T_1 \approx 20$ ms; Figure 3D) whose relaxation properties and shift are similar to those in the His(E7) N_ϵH, observed for

(52) Bardakdjian-Michau, J.; Galacteros, F.; Craescu, C. T. *Biochim. Biophys. Acta* **1990**, *1041*, 250−253.

(53) Russu, I. M.; Ho, N. T.; Ho, C. *Biochim. Biophys. Acta* **1987**, *914*, 40−48.

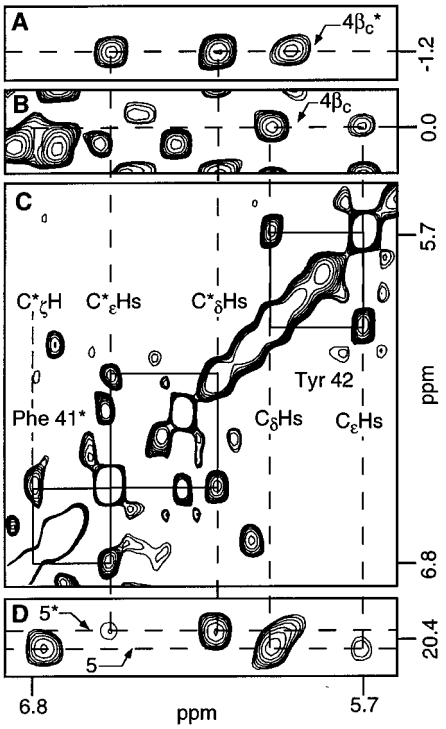

Figure 8. Portions of the NOESY ($\tau_m = 35$ ms) (A, B, D) and clean-TOCSY ($\tau_m = 15$ ms) (C) spectra for metHbACN in ^2H_2O, 20 mM in NaCl at 45 °C, identifying the C7 aromatic side chain contact to the heme 4-vinyl (A, B) and 5-CH_3 (D) which provides the subunit differentiation for the two subunits (three-spin aromatic Phe(C7) in α- and Tyr two-spin aromatic C7 in β-subunits.

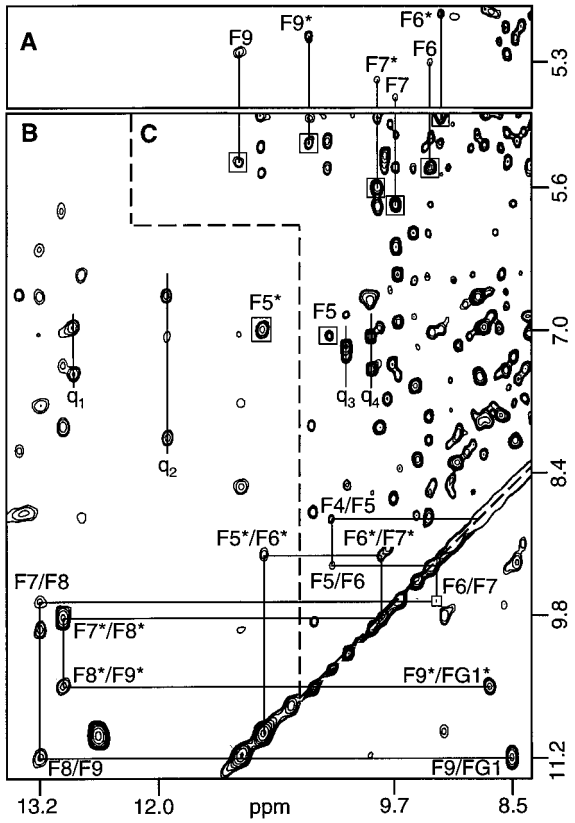

Figure 9. Fingerprint region of the SCUBA-TOCSY ($\tau_m = 20$ ms) (A), NOESY ($\tau_m = 35$ ms) (B), and 1:1 NOESY ($\tau_m = 40$ ms, without solvent saturation) (C), for metHbACN on 90% ^1H_2O:10% ^2H_2O, 20 mM in NaCl at 37 °C. The $N_i - N_{i+1}$ dipolar connectivity for residues F5−FG1 are traced out in B and C.

all His(E7)-containing metMbCN.[22,54] The extreme relaxation properties of both the $N_\epsilon H$ and $C_\delta H$ of His(E7), together with the spectral crowding and the need to carry out the NMR experiment in ^1H_2O, have prevented the detection of the NOESY cross peak to the His(E7) $C_\delta H$ that would establish the identity as $N_\epsilon H$ of His(E7) as well as the subunit origin of the labile proton.

A pair of TOCSY-detected isopropyl fragments exhibits methyl NOESY cross peaks to the His(E7) $C_\delta H$ which identify the terminus of Leu(B10) in the respective subunits, and two aromatic protons in the α-subunit with NOESY cross peaks His-(E7) $C_\delta H$ and $6H_\beta$s locate Phe(CD4). NOESY cross peaks from obvious methyls to the heme 5-CH_3, $6H_\alpha$s are unique to the terminus of Leu(FG3), while similar NOESY cross peaks to 1-CH_3 in the β-subunit locate $C_\beta H$-$C_{\gamma 2}H_3$ of Val(H15). Weak NOESY cross peaks from the β-subunit, but not α-subunit 1-CH_3, to several aromatic protons identify Phe(F1) (7.35, 6.75 ppm) and Phe(E15) (6.58 ppm) which are replaced by aliphatic residues in the α-subunit. Strong NOESY cross peaks from the 8-CH_3 to a strongly upfield-shifted proton identify the likely Lys(E10) $C_\beta H$ in each subunit. Further unambiguous assignments were complicated by severe spectral congestion. Chemical shifts are listed in Table 2.

(E) Magnetic Axes. A plot of the slopes of the chemical shift in a Curie plot against δ_{dip}(obsd) (data not shown; see the Supporting Information) yields a good correlation for all protons used as input, as well as the majority of the other protons, indicating that all have well-defined positions relative to the heme[17] (data not shown; see the Supporting Information). The Leu(FG3) $C_\delta H_3$s, on the other hand, and, to a lesser degree, the Leu(B10) $C_\delta H_3$, exhibited significant deviation, with a slope of the wrong sign for the former, which can be taken as evidence for alternate orientations in the heme pocket. The magnetic axes for each of the subunits were determined using the definitively assigned nonlabile proton resonance in Table 1 for all but the heme and axial His(F8) protons that exhibit dipolar shifts.[55] These dipolar shifts are reflected in either strong temperature dependence of the shift and/or a shift significantly different than observed in HbACO or calculated using the HbACO structure. In each case, a three-parameter search for the three Euler angles using the available anisotropies for isoelectronic metMbCN at 37 °C, $\Delta\chi_{ax} = 1.97 \times 10^{-9}$ mol^{-1} and $\Delta\chi_{rh} = -0.39 \times 10^{-9}$ mol^{-1},[18,56] produced an excellent fit with a low residual error function. The relevant parameters resulting for the two subunits at 37 °C are $\alpha = 30°$ (tilt direction of the major axis), $\beta = 12°$ (tilt magnitude from the heme normal), $\kappa \approx \alpha + \gamma = 40°$ (projection of rhombic axes on heme plane) and residual error $F/n = 0.12$ ppm^2 for the α subunit, and $\alpha = 0°$, $\beta = 10°$, $\kappa = 30°$, and residual $F/n = 0.12$ ppm^2 for the β-subunit. The excellent correlation between δ_{dip}(obsd) and δ_{dip}(calcd) in the two subunits is shown in Figure 10 for the α (open markers) and β (solid markers) subunits. Analysis of more extensive NMR data on metMbCN[18] has indicated that the uncertainty in the three angles of interest are ±10° for α and κ, and ±1° for β. Hence, the magnetic axes are similar in the two subunits.

(54) Lecomte, J. T. J.; La Mar, G. N. *Eur. Biophys. J.* **1986**, *13*, 373−381.

(55) The δ_{dip}(obsd) used as input are $C_\alpha H$ and $C_\beta H$ of Val(E11), $C_\alpha H$ and $C_\beta H_3$ of Ala(E14), $C_\alpha H$ and $C_\beta H$s of Leu(F4), $C_\alpha H$s of Ser(F5) and Asp/Glu(F6), $C_\alpha H$ and $C_\beta H$s of Ala/Cys(F9), $C_\alpha H$, $C_\beta H$, and $C_\gamma H_3$ of Val-(FG5), and ring protons of Phe(CD1) and Phe(G5).

(56) Nguyen, B. D. Ph.D. Dissertation, University of California−Davis, 1997.

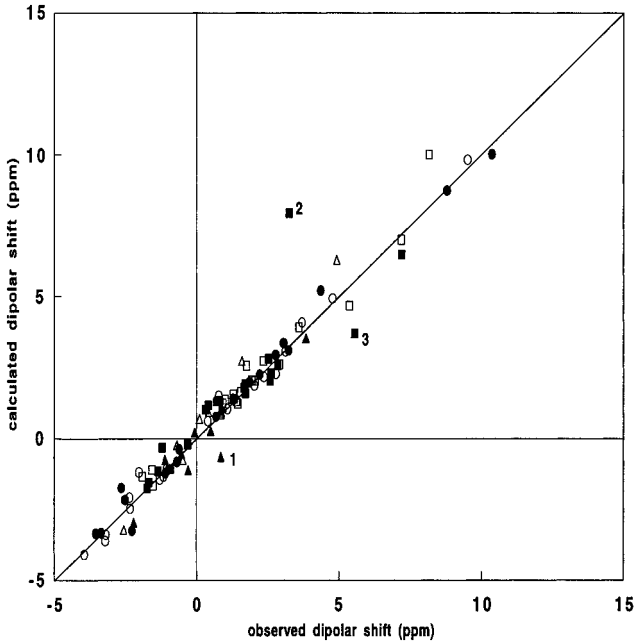

Figure 10. Correlation between observed and calculated dipolar shifts for the α-subunit (open marker) and β-subunit (closed marker) for the optimized magnetic axes $\alpha = 30°$, $\beta = 12°$, $\kappa = 40°$ for the α-subunit and $\alpha = 0°$, $\beta = 10°$, $\kappa = 30°$ for the β-subunit with the $\Delta\chi_{ax} = 1.97 \times 10^{-9}$ m^3/mL, $\Delta\chi_{ax} = -0.39 \times 10^{-9}$ m^3/mL obtained from metMbCN. The signals used to determine the magnetic axes are given as circles, other assignments for which the δ_{dip}(obsd) correlated with Curie slope are shown in squares, and tentative assignments are shown as triangles. The signals for which δ_{dip}(obsd) did not correlate well with the Curie slope, likely due to mobile side chain protons, are labeled #1 Leu(FG3) $C_\delta H_3$ and #2, #3, $C_\delta H_3$s of Leu(B10).

Discussion

Efficacy of the 2D NMR. The clean-TOCSY variant provided[32] dominant scalar correlation cross peaks for all expected heme side chains (four vinyls, four propionates) in spite of a line width of 70 Hz and $T_1 \approx 90$ ms for the propionate H_αs. ROESY cross peaks of opposite sign, particularly for geminal protons, were observed at weaker spin-lock fields and when using normal TOCSY. Even the TOCSY cross peaks between the ∼20 ms, ∼100 Hz Phe(CD1) $C_\zeta H$ and C_ϵHs were weakly detectable (Figure 5), which constitutes the pair of spin-coupled protons closest to the iron. The necessary NH-C_αH TOCSY peaks even for the residue backbone closest to the iron, His(F8) exhibits good intensity cross peaks, a surprising observation for a primarily helical 65 kDa protein. Hence, the prospects for further sequence-specific assignments are very reasonable for metHbACN and likely other isoelectronic tetrameric Hb.[57]

Surprisingly, COSY spectra exhibit little evidence for cross correlation contributions in 65 kDa metHbACN,[46] in contrast to the findings for the smaller, isoelectronic cyanide complex of ∼44 kDa horseradish peroxidase, HRP-CN, where cross correlation resulted in a large number of MCOSY cross peaks between non-spin-coupled but spatially close proton pairs.[58] The minimal cross correlation contributions in metHbACN are qualitatively documented by the weak COSY cross peak between the only ∼2 Hz spin-coupled vinyl H_βs and by the absence of COSY cross peaks for proton pairs that also do not exhibit TOCSY cross peaks (data not shown; see the Supporting Information). The heme iron paramagnetic relaxivity is about the same in metHbACN and HRP-CN,[59] so that the ∼30% larger size for the former protein should have made cross correlation more problematic.[46] A possible origin of the effectiveness of TOCSY and the suppression of cross correlation in metHbACN is its greater internal flexibility as supported by much faster labile proton exchange with water in metHbACN than HRP-CN.[60]

The presence of secondary NOEs to geminal ($r_{ij} \approx 1.8$ Å) protons after ∼5 ms and to vicinal ($r_{ij} \approx 2.5$ Å) proton after ∼10 ms, as observed for the 5-CH_3-6H_αs in Figure 6A and as observed to Phe(CD1) $C_\delta H$ and Phe/Tyr(C7) C_ϵHs in Figure 6B, dictates the use of relatively short mixing times to obtain distance from primary NOEs. NOESY maps exhibit sufficient sensitivity for protons in the immediate vicinity of the heme even for the short mixing times needed to provide reasonable estimates for cross peak volumes as previously found for 44 kDa HRP-CN.[59] The combination of the present TOCSY and NOESY experiments provides the assignments for the target residues depicted in Figure 1 in a manner that is not much more complicated than previously successfully applied for monomeric metMbCN, metHbCN.[18−22] Most importantly, the properly tailored available 2D NMR methods allow the definitive assignment of the key components in the heme pocket proposed to be modulated by the binding of allosteric effects or to involve the mechanisms of cooperativity,[2,9,61,62] the F-helices, His(E7), Val(E11), Val(FG5), Phe/Tyr(C7) in both subunits, and Cys(F9) in the β-subunit.

Subunit/Sequence-Specific Assignments. The subunit origin of heme assignments deduced by 2D NMR alone confirm, and greatly extend, assignments obtained earlier by tedious subunit-specific heme deuteration,[28] or valency hybrids.[26] The individual subunits origins from residues are readily observed without recourse to either isotope labeling or a crystal structure simply by observing the difference in key heme contacts that are predictable solely from sequence homology with other globins and the invariant Mb fold that conserves numerous heme contacts to residues at specific helical or loop positions. While degeneracy can be much more of a problem at any one temperature than in monomeric globins, the use of variable temperature data allow the necessary distinction for the presently assigned residues.

The facility with which the F-helix backbone can be traced for each subunit owes its surprising success to the significantly increased dispersion afforded by the dipolar shifts. While δ_{dip}(calcd) is to low-field for residues F4-F9 C_αHs and N_pHs (∼1 to ∼5 ppm), their variable magnitude increases both the N_pH and C_αH dispersion by ∼4 ppm relative to a diamagnetic analog. The majority of the F4−F9 side chain protons are similarly predicted to exhibit significant dipolar shifts which should facilitate their ultimate assignments; their unambiguous assignment at this stage is incomplete because of severe spectral congestion near the water signal. The δ_{dip}(calcd) values for the E-helix backbone are much smaller (with the largest ∼1.5 ppm for Ala(E14)) than those for the F-helix (to ∼5 ppm), making the resolution and identification of the E-helix backbone more difficult. However, it is expected that even this problem

(57) McGourty, J. L.; La Mar, G. N.; Smith, K. M.; Ascoli, F.; Chiancone, E.; Pandey, R. K.; Singh, J. P. *Eur. J. Biochem.* **1989**, *184*, 53−61.
(58) Chen, Z.; de Ropp, J. S.; Hernández, G.; La Mar, G. N. *J. Am. Chem. Soc.* **1994**, *116*, 8772−8783.
(59) Sette, M.; de Ropp, J. S.; Hernández, G.; La Mar, G. N. *J. Am. Chem. Soc.* **1993**, *115*, 5237−5245.
(60) de Ropp, J. D.; La Mar, G. N. *Plant Peroxidases: Biochemistry and Physiology*; Welinder, K. G., Rasmussen, S. K., Penel, C., Greppin, H., Eds; University of Geneva Press: Geneva, Switzerland, 1993; pp 45−55.
(61) Perutz, M. F. *Quart. Rev. Biophys.* **1989**, *22*, 139−236.
(62) Bunn, H. F.; Forget, B. G. *Hemoglobin: Molecular, Genetic and Clinical Aspects*; Saunders: Philadelphia, 1986.

can be overcome by tedious, but needed, variable-temperature studies at high field strength.

Magnetic Properties and Electronic Structure of the Heme. The magnetic axes predict relatively small δ_{dip} for the heme pyrrole substituents ($\delta_{dip} < 5$ ppm), indicating that the hyperfine shifts are dominated by the contact interaction. The pattern of large 1-CH_3, 2-vinyl, 5-CH_3, 6-H_α and small 3-CH_3, 4-vinyl, 7H_α, 8-CH_3 contact shifts is indicative of an orbital ground state that results in spin delocalization into one pair of *trans*-pyrroles (pyrroles A,C), as determined largely by the orientation of the axial His.[16] The observation of Curie-like temperature dependence for the 1-CH_3, 5-CH_3, and 6H_α peaks, but similar anti-Curie behavior for the 3-CH_3, 8-CH_3, and 7H_α peaks, is consistent with thermal population of the excited orbital state that results in spin delocalization also to the pyrroles B,D.

The magnetic axes result in rhombic axes $\kappa = 30-40°$ which are close to the orientation of the axial His(F8) imidazole plane in the HbACO structure.[5] The major magnetic axis is tilted from the heme normal to the same degree ($\sim$12°) and in a similar direction in the α- and β-subunits. The magnetic axes, moreover, correctly predict the position of several resonances for which only tentative assignments could be made (*i.e.*, Lys-(E10) C_βH, methyl of Val(E11)), establishing their utility as a guide for assignments. At the same time, the absence of a correlation of Curie slope with δ_{dip}(obsd) for several aliphatic side chain termini (*i.e.*, Leu(FG3) and Leu(B10)) provides evidence for multiple side chain orientations.[17] The magnetic axes can be expected to provide a wealth of structural information on the distal pocket of HbA upon systematic mutagenesis of the relevant distal residue, as has been reported for the analogous metMbCN.[18−21]

Molecular Structure of Subunit Heme Pockets. The strong correlation between δ_{dip}(obsd) and δ_{dip}(calcd) for the assigned heme resonances indicates that the distal pocket geometry, in most respects, is essentially the same as that in the HbACO crystal.[5] The resolved residues in metHbACN are the same as those in metMbCN with very similar chemical shift.[37] For His-(E7) in metHbACN, only one signal could be detected outside the diamagnetic spectral window (Figure 3D) which exhibits the unique relaxation properties of the N_ϵH that is expected to provide the hydrogen bond to the ligated cyanide. The same signal for the other subunit[63] cannot be resolved, or its exchange with bulk solvent may be much more rapid in one than the other subunit; it is also possible the ring labile proton may reside on the N_δ rather than on N_ϵ of the His(E7) ring, as in MbCO.[64] The NOESY rise curves in Figure 6B correctly show primary NOEs from the 5-CH_3 to the ring H_ϵs ($r_{ij} \approx 3$ Å), but secondary to H_δs ($r_{ij} \approx 5$ Å) for Phe(CD1), and primary NOE to ring H_δs ($r_{ij} \approx 3.5$ Å) and secondary to H_ϵs ($r_{ij} > 5$ Å) for Phe/Tyr(C7), as is expected from the relative distances in the HbACO structure.

The HbACO crystal structure shows that the iron-bound carbonyl is bent/tilted similarly from the heme in the direction of the β-*meso*-position in both subunits, with the oxygen off the heme normal by comparable degrees in the two subunits.[5] The major magnetic axes in the two subunits are tilted approximately in the same direction and to the same degree as for the Fe−CO vector in HbACO, and, by implication, argue for a tilted Fe−CN vector toward the β-*meso*-H in each subunit. As is the case in MbCO[4] and metMbCN,[17,18] the tilt of the Fe−CO and Fe−CN can be rationalized by the steric influence of the highly conserved Val(E11).

The 7-propionate groups in both subunits and the 6-propionate in the α-subunit exhibit similar shifts for the two C_αHs and primary NOEs for one C_αH and one C_βH to the adjacent heme methyl which are consistent with their extended orientations in crystal structures.[65] For the 6-propionates in the β-subunit, the 5-CH_3 exhibits primary NOEs to one C_αH (Figure 6A) but not to either C_βH (data not shown; see the Supporting Information), indicating that the 6-propionate terminus is oriented away from the 5-CH_3. However, this turning away from the 5-CH_3 is not as severe as found in the HbACO crystal structure[5] where its orientation places both C_αH and C_αH′ similarly close to 5-CH_3. The rise curves involving the 6-propionate H_αs in the two subunits also exhibit some important differences. First, the rise curves from 6H_α to the 5-CH_3 differs significantly, with a much weaker initial slope, and hence smaller cross-relaxation rate, σ ($\propto r_{ij}^{-6}$), in the β- than in the α-subunit. In part, the smaller σ could arise from the rotation of the $C_\alpha H_2$ group compared to that of the α-subunit, as indicated by the spread of the largely contact shift; however, the 5-CH_3−6H_α distance cannot increase by the $\sim$15% expected by the factor of $\sim$2 smaller σ. It is also noted that the 6C_αH−6C_αH′ rise curve in the β-subunit is also not as steep as in the α-subunit,[66] in spite of necessarily identical $r_{ij} \approx 1.8$ Å. It is observed that the two subunits exhibit essentially identical rise curves for pairs of immobile protons such as the Ala(E14) C_αH-$C_\beta H_3$ groups (data not shown; see the Supporting Information). The lower initial slope in the 6C_αH−6C_αH′ rise curve in the β-subunit must therefore reflect considerable oscillatory mobility of the side chain that reduces the effective σ with the 5-CH_3. It is of interest that the 6-propionate in the β-subunit is found with different orientation in the various Hb crystal structures,[5,65] while the α-subunit 6-propionate, as well as the 7-propionates of both subunits, have well-defined positions.

Steric interaction with the adjacent heme methyl and *meso*-H preclude coplanarity between a vinyl and the heme;[67] however, protein constraints modulate the relative stability of the *cis* (vinyl H_βs near adjacent methyl) and *trans* (vinyl H_α near adjacent methyl) orientations. The intraheme NOESY pattern for the 2-vinyl group reflect a mobile side chain that exists primarily in the *cis* orientation ($H_{\beta t}$-1CH_3 and 2H_α-α-*meso*-H cross peaks), but also weakly populates the *trans* oriented (weak 2H_α-1CH_3 and $H_{\beta t}$-3CH_3 NOESY cross peaks). Both 4-vinyl groups exhibits strong 4-H_β-3CH_3 and 4H_α-5CH_3 NOESY cross peaks and no detectable 4$H_{\beta t}$-5CH_3 NOESY cross peaks which are indicative of a dominant *cis* orientation; a stronger 4H_α-5CH_3 NOESY cross peak in the β- than α-subunit suggests that the 4-vinyl may be slightly more out-of-plane in the α-subunit. The observation of a moderate intensity 4$H_{\beta t}$ to Val(FG5) $C_{\gamma 1}H_3$ NOESY cross peaks only in the β-subunit, and a 4H_α to Val-(FG5) $C_{\gamma 2}H_3$ NOE much more stronger (compare Figure 7B−D) in the α-subunit, moreover, shows that the out-of-plane positions of the 4-vinyl groups are in *opposite directions in the two subunits*.

The proposed mechanism of cooperativity involves communication between the αβ subunit interface and the heme via the Val(FG5) interaction with the 4-vinyl group, and hence, it can be expected that the vinyl contacts will serve as sensitive

(63) From the comparison with preliminary data on the separated subunits α-HbACN and β-HbACN, the strongly relaxed ($T_1 \approx 20$ ms) labile proton near 17 ppm in the spectrum of HbACN is likely to come from the N_ϵH of the His(E7) ring in the α-subunit.

(64) Hanson, J. C.; Schoenborn, B. P. *J. Mol. Biol.* **1981**, *153*, 117−146.

(65) Silva, M. M; Rogers, P. H.; Arnone, A. *J. Biol. Chem.* **1992**, *267*, 17248−17256. Smith, F. R.; Simmons, K. C. *Proteins: Struct., Funct., Genet.* **1994**, *18*, 295−300.

(66) The line width for the 6H_α peak in the two subunits differ slightly (by 10−15%), but cannot account for the factor of $\sim$2 difference in initial slopes in the rise curves.

(67) Kalsbeck, W. A.; Ghosh, A.; Pandey, R. K.; Smith, K. M.; Bocian, D. F. *J. Am. Chem. Soc.* **1995**, *117*, 10959−10968.

probes of such interactions.[10] Recent studies have shown that constraints on distance of the F-helix to the heme plane account for a majority, but not all, of the energy of cooperativity,[68] with differential interactions between ligand and the Val(E11) and His(E7) side chains likely also contributing.[6] The present study indicates that ^{1}H 2D NMR spectroscopy is very well suited for directly monitoring changes in both F-helix−heme and Val(FG5)−heme contacts in the cyanomet subunit of a valency hybrid of HbA that is capable of undergoing the allosteric transition. Changes in distal interactions would be sensed by perturbations of the magnetic axes as well as by perturbed dipolar contacts and/or paramagnetic relaxivity.

(68) Barrick, D.; Ho, N. T.; Simplaceanu, V.; Dahlquist, F. W.; Ho, C. *Nat. Struct. Biol.* **1997**, *N1*, 78−83.

Acknowledgment. The authors are indebted to B. Nguyen and E. Chien for valuable discussion and to J. S de Ropp for experimental assistance. This research was supported by grants from the National Institutes of Health (HL 16087 and GM 26226).

Supporting Information Available: Six figures, temperature dependence on NMR spectra of metHbACN in ^2H_2O, magnitude COSY and NOESY connections for Val(FG5), slices of the NOESY spectrum through the 5-CH_3, NOESY cross peaks between heme protons, correlation between Curie slopes and observed dipolar shift, and NOESY rise curves for Ala(E14) (6 pages). See any current masthead page for ordering and Internet access instructions.

JA9722133